PNAS

Supporting Information for

Prestin's fast motor kinetics is essential for mammalian cochlear amplification

Satoe Takahashi, Yingjie Zhou, Takashi Kojima, Mary Ann Cheatham, and Kazuaki Homma

Address correspondence to: Kazuaki Homma
Email: k-homma@northwestern.edu

This PDF file includes:

Figures S1 to S6

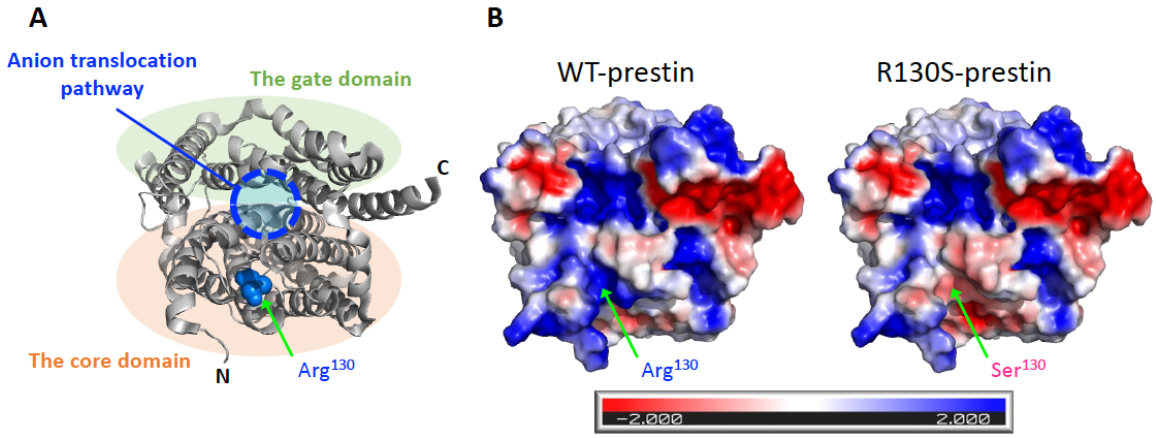

Fig. S1. An intracellular view of the prestin protein. (**A**) A ribbon representation of the transmembrane domain of a human prestin protomer (PDB ID: 7LGU). N, N-terminus. C, C-terminus. The cytosolic domains and a bound chloride ion are not shown. (**B**) Surface electrostatic potential calculated by PyMOL for WT and R130S variant (modeled by PyMOL). Blue signifies positive charge.

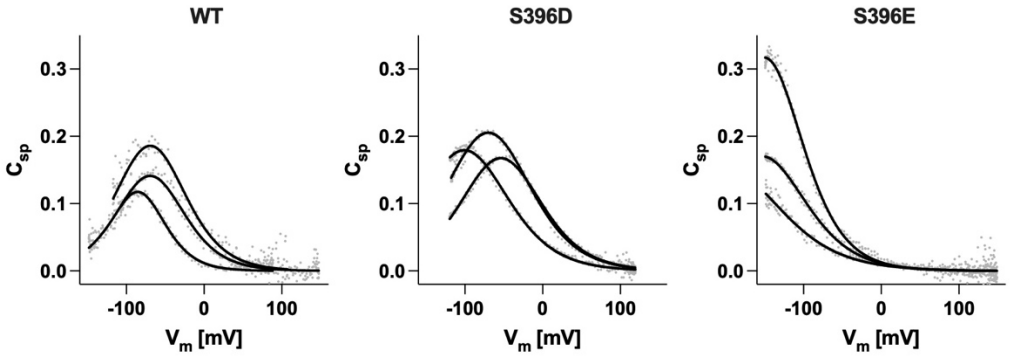

Fig. S2. NLC recordings for gerbil prestin constructs. NLC was measured in HEK293T cells bathed in a solution containing (mM): 120 NaCl, 20 TEA-Cl, 2 $CoCl_2$, 2 $MgCl_2$, 10 HEPES (pH 7.4). Recording pipettes were filled with an intracellular solution containing (mM): 140 CsCl, 2 $MgCl_2$, 10 EGTA, and 10 HEPES (pH 7.4). Solid lines indicate two-state Boltzmann curve fits. NLC data are corrected for cell size ($C_{sp} = (C_m - C_{lin})/C_{lin}$), as larger cells tend to express larger amounts of the prestin protein. Note that the NLC of S396D-prestin is qualitatively more similar to WT-prestin than to S396E-prestin. The difference in NLC between S396D-prestin and S396E-prestin may be ascribed to the difference in the length of the side chains, which would place a negative charge at slightly different positions within the anion binding pocket.

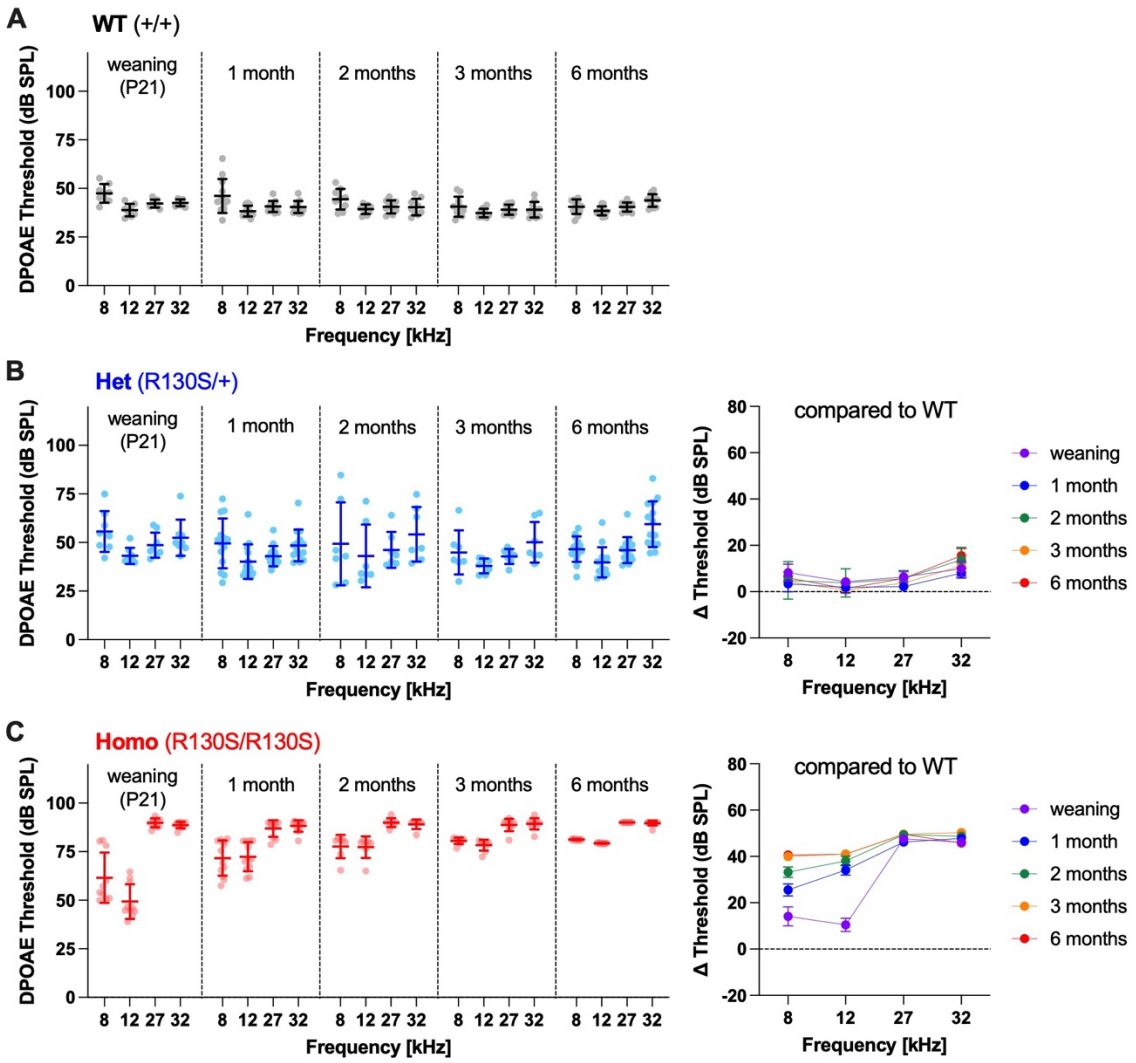

Fig. S3. Age dependence of DPOAE thresholds in R130S-prestin KI mice. DPOAE thresholds were determined for WT littermates (*Slc26a5*$^{+/+}$, **A**), heterozygotes (*Slc26a5*$^{R130S/+}$, **B**), and homozygotes (*Slc26a5*$^{R130S/R130S}$, **C**) at various ages indicated in the figures. Right panels show differences in thresholds with respect to the WT controls. Horizontal solid lines indicate means and standard deviations (left panels) or propagated errors (right panels) calculated from standard errors of the original threshold data (left panels).

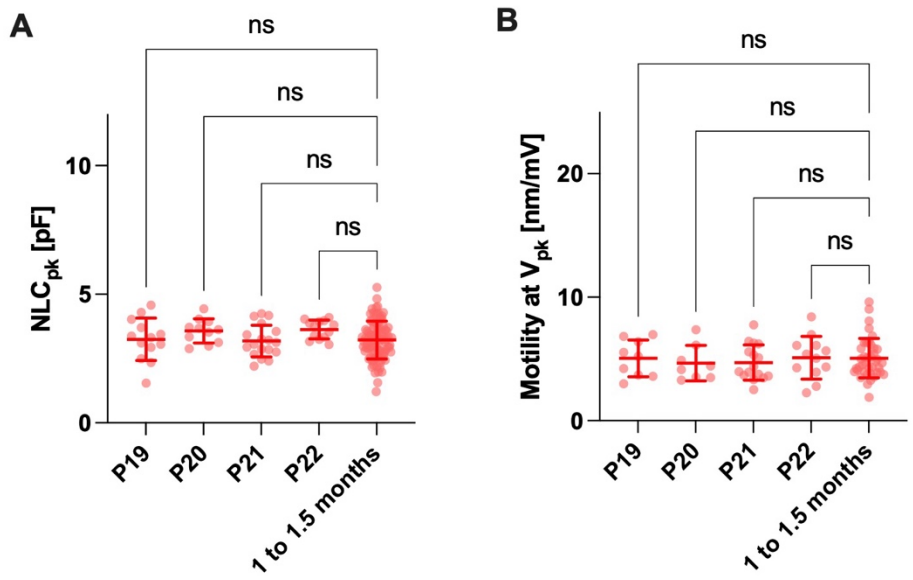

Fig. S4. Electrophysiological properties of OHCs isolated from R130S-prestin homozygous mice at various ages. NLC (**A**) and electromotility (**B**) were measured as in Fig. 5. Short horizontal lines indicate the means and standard deviations. The *p* values were computed by one-way ANOVA followed by the Tukey's multiple comparison procedure. ns, $p \geq 0.05$.

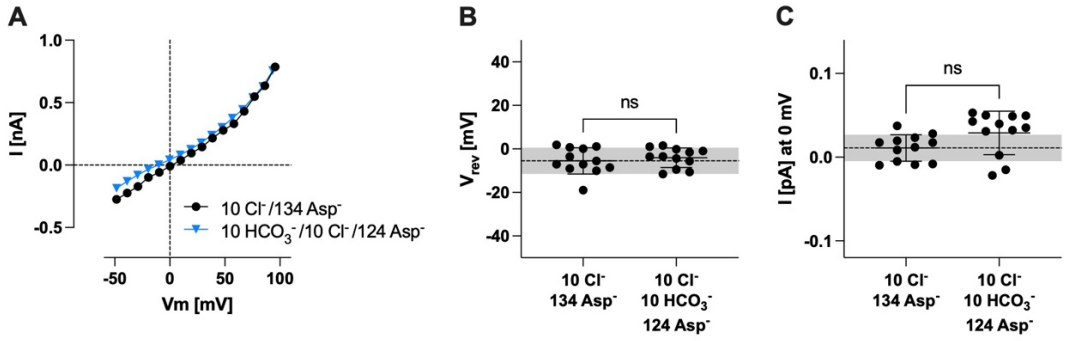

Fig. S5. Whole-cell electrophysiological $2HCO_3^-/Cl^-$ antiport assay for wild-type OHCs. The bath solution contained 148 mM Cl^-, while the intracellular (pipette) solution contained 10 mM Cl^- with or without 10 mM $NaHCO_3$. Aspartate (Asp^-) was used to partially replace intracellular Cl^-. The bath solution and the intracellular solution without $NaHCO_3$ were equilibrated with ~400 ppm of atmospheric CO_2. Thus, these solutions were estimated to contain ~150 μM HCO_3^-. The Nernst equilibrium potentials are calculated to be -69 mV for chloride (E_{Cl}) and +106 mV (with 10 mM intracellularly added $NaHCO_3$) or -69 mV (without $NaHCO_3$ but with 150 μM HCO_3^-) for bicarbonate (E_{HCO3}). The reversal potential (V_{rev}) for $2HCO_3^-/Cl^-$ electrogenic antiport is computed to be +281 mV ($V_{rev} = 2E_{HCO3} - E_{Cl}$). (**A**) Examples of whole-cell voltage clamp recordings with (blue triangle) and without (black circle) intracellularly added $NaHCO_3$. (**B**) A summary of V_{res}: -4.0 ± 4.5 mV (mean ± SD, n=12) vs. -5.5 ± 6.0 mV (mean ± SD, n=12) for with vs. without intracellularly added $NaHCO_3$, respectively ($p > 0.05$). Note that inclusion of $NaHCO_3$ in the intracellular solution did not result in positively shifted V_{res}. (**C**) A summary of whole-cell currents measured at 0 mV holding potential. Although large inward (negative) currents at 0 mV were anticipated for the intracellular solution containing 10 mM $NaHCO_3$, this was not the case: 0.029 ± 0.025 nA (n = 12) vs. 0.011 ± 0.016 nA (n = 12) (mean ± SD) for with vs. without intracellularly added $NaHCO_3$, respectively ($p > 0.05$).

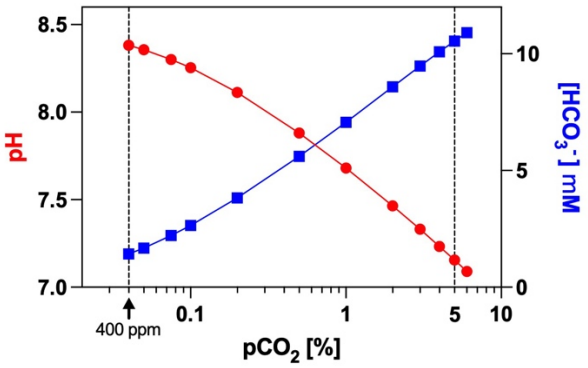

Fig. S6. The dependence of pH and bicarbonate concentration on the partial pressure of carbon dioxide (pCO_2). Computations were carried out using the following pK values: 1.47 ($[H_2CO_3^*]/pCO_2$), -0.143 ($[H^+][HCO_3^-]/[NaHCO_3]$), 6.35 ($[H^+][HCO_3^-]/[H_2CO_3^*]$), 10.33 ($[H^+][CO_3^{2-}]/[HCO_3^-]$), 1.99 ($[H^+][Asp]/[Asp^+]$), 3.90 ($[H^+][Asp^-]/[Asp]$), 9.90 ($[H^+][Asp^{2-}]/[Asp^-]$), 15.7 ($[H^+][OH^-]/[H_2O]$), 7.48 ($[H^+][HEPES^-]/[HEPES]$). $H_2CO_3^*$ denotes the equilibrium mixture of the aqueous carbon dioxide and carbonic acid. Note that these computations are for the 10 mM $NaHCO_3$-containing intracellular solution.